Hindawi
Journal of Chemistry
Volume 2019, Article ID 9568360, 15 pages
https://doi.org/10.1155/2019/9568360

Research Article

Dissolution and Solubility of the Synthetic Natroalunite and the Arsenic-Incorporated Natroalunite at pH of 2.00–5.60 and 25–45°C

Yinian Zhu,[1] **Huiling Xuan**,[1] **Yanpeng Liang**,[2] **Qiming Yan**,[1] **Zongqiang Zhu**,[1] **Zhangnan Jiang**,[1] **Lihao Zhang**,[2] **Huili Liu**,[1] **and Shen Tang**[2]

[1]*College of Environmental Science and Engineering, Guilin University of Technology, Guilin 541004, China*
[2]*Guangxi Key Laboratory of Environmental Pollution Control Theory and Technology, Guilin University of Technology, Guilin 541004, China*

Correspondence should be addressed to Yinian Zhu; zhuyinian@glut.edu.cn and Yanpeng Liang; liangyanpeng@glut.edu.cn

Received 16 August 2019; Accepted 16 October 2019; Published 3 November 2019

Academic Editor: Sedat Yurdakal

Arsenic is very harmful to most living organisms. The solubility data of As-containing compounds are significant in geoscience and environmental science. The arsenic-incorporated natroalunite precipitation has been proposed to eliminate arsenic from water, both for industrial practice and remediation of polluted areas. Unfortunately, only few works have been made on partial arsenic incorporation in natroalunite and the thermodynamic data for natroalunite and arsenic-incorporated natroalunite now are still lacking. Moreover, the dissolution mechanisms of arsenic-incorporated natroalunites have never been studied. In the present work, the dissolution of the synthetic natroalunite $[Na_{0.93}(H_3O)_{0.61}Al_{2.82}(SO_4)_2(OH)_6]$ and the synthetic arsenic-incorporated natroalunite $[Na_{0.88}(H_3O)_{2.44}Al_{2.35}(AsO_4)_{0.38}(SO_4)_{1.62}(OH)_6]$ at 25°C, 35°C, and 45°C was experimentally examined in HNO_3 solution (pH of 2.00 and 4.00) and pure water. The characterizations confirmed that the solids showed no recognizable change after dissolution. All dissolutions underwent a pH variation, which was caused by a great depleting of H_3O^+/OH^- ions, typically at the reaction beginning. The dissolution in H_3O^+ medium proved to be near-stoichiometric within the short beginning period, and the dissolved Na^+, Al^{3+}, SO_4^{2-}, and AsO_4^{3-} concentrations were stoichiometric according to the initial solids and then appeared to be nonstoichiometric with the Na/SO_4 mole ratios higher and the Al/SO_4 and AsO_4/SO_4 mole ratios lower than the stoichiometry until the experimental end, indicating that the components were released from solid to solution preferentially after the following order: Na^+ $(H_3O^+) > SO_4^{2-} > AsO_4^{3-} > Al^{3+}$. From the experimental results under the condition of initial pH 2.00 and 25°C, the solubility products $[K_{sp}]$ and the Gibbs free energies of formation $[\Delta G_f^\circ]$ were calculated to be $10^{-81.02\pm0.33}$~$10^{-81.04\pm0.27}$ and -4713 ± 2 to -4714 ± 1 kJ/mol for the natroalunite and $10^{-92.30\pm0.30}$~$10^{-92.41\pm0.37}$ and -5078 ± 2 to -5079 ± 2 kJ/mol for the arsenic-incorporated natroalunite, respectively. The thermodynamic quantities, ΔG°, ΔH°, ΔS°, and ΔC_p°, were determined to be 462303.43 J/K·mol, 122466.83 J/mol, −1140.39 J/K·mol, and 4280.13 J/K·mol for the natroalunite dissolution reaction at initial pH 2.00 and 25°C and to be 526925.48 J/K·mol, 159674.76 J/mol, −1232.38 J/K·mol, and 1061.12 J/K·mol for the dissolution of the arsenic-incorporated natroalunite at initial pH 2.00 and 25°C, respectively.

1. Introduction

The element arsenic (As) is very harmful to most animals and plants [1, 2]. Its high levels in air, water, and soil can result from a combination of human activities and natural processes [3, 4]. Arsenic is commonly found in mine waters and solid wastes from nonferrous metal mining and metallurgy, and many researchers have made efforts to develop techniques to eliminate and stabilize this toxicant, but it is still a very great challenge for nonferrous metal industries [5, 6]. Information about the processes controlling arsenic in environments is needed to predict its distribution in different phases. The solubility data of As-containing compounds are significant in geoscience and environmental science [7].

The precipitation of metal arsenates is an important process controlling arsenic levels in natural environment and industrial discharges. Acid mine drainage and

industrial wastewaters are generally treated by adding low-cost calcium oxide/hydroxide to adjust effluent pH and reduce the arsenic release into natural waters through the formation of low-soluble calcium arsenate precipitates [8–12], which nevertheless are not stable and may release arsenate ions in some water environments [12]. Scorodite ($FeAsO_4{\cdot}2H_2O$), one of the most frequent arsenate minerals in the oxidizing belt of nonferrous metal deposits, is considered to control the As levels in mining areas and also extensively studied for arsenic removal and residue-storage [13, 14], assuming that it is comparatively insoluble, but in fact, all Fe/Al arsenates are metastable and tend to form hydroxides and release arsenic remarkably into the aqueous environment [15–17]. Besides, most acidic mine drainages and metallurgical discharges are sulfate-rich and arsenic-containing wastewaters, for which it is especially interesting to eliminate arsenic as crystalline sulfate-arsenate precipitates such as the $Fe(SO_4)_x(AsO_4)_{1-x}(OH)_x{\cdot}(1-x)H_2O$ compounds with the lower arsenic release in leaching test than $FeAsO_4{\cdot}2H_2O$ [18].

Recently, many scholars aim to study the AsO_4-for-SO_4 replacement in natroalunite [$NaAl_3(SO_4)_2(OH)_6$], a member of the alunite supergroup [$AB_3(TO_4)_2(OH,H_2O)_6$] that exists in oxidizing, acidic, and S/Al-rich environments, and it is very common and extremely stable in nature [19, 20]. The ideal natroalunite has a common formula of $NaAl_3(SO_4)_2(OH)_6$, made up of linear tetrahedral-octahedral-tetrahedral (T-O-T) laminas, where the Na^+ ion sites with an $AO_6(OH)_6$ icosahedra coordination and the Al^{3+} and SO_4^{2-} ion sites with slightly distorted AlO_6 octahedra (O) and SO_4 tetrahedral (T) coordinations, respectively [21]. The A sites are commonly filled by K^+, Na^+, and H_3O^+, the B sites by Fe^{3+} and Al^{3+}, and the TO_4 sites by SO_4^{2-}, PO_4^{3-}, and AsO_4^{3-}, respectively. Multiple replacements are possible due to the charge balance by the coupled replacement at different sites, the OH/TO_4 protonation, and the cationic vacancy [22, 23]. Therefore, the alunite group minerals may act as a provisional store for the substituted toxic metal(loid)s and then release these toxic metal(loid)s when the minerals dissolve in water [19, 24]. Since so many different ions can substitute into the natroalunite lattice, the arsenic-incorporated natroalunite (As-natroalunite) precipitation has been proposed to eliminate arsenic from water, both for industrial practice and remediation of polluted areas [22, 25].

The incorporation of AsO_4 in the SO_4 sites of alunite can achieve 15 mol% [23, 26]. Moreover, the alunite supergroup minerals are more stable than the jarosite supergroup minerals since the trivalent aluminum ion is unreducible in the anoxic milieu. Their solubility, stability, and mobility depend not only on the solution pH but also on the degree of isomorphous incorporation in the alunite structure [22]. Lately, the replacement of arsenate for sulfate in natroalunite is examined by some scholars [27–30]. Nevertheless, few works have been carried out on the arsenic incorporation in natroalunite. The hydrothermal-precipitated natroalunite could incorporate about 8 mol% AsO_4 in its structure and release <1 mg/L As in the leaching tests at pH 4-5 for 6 months [30]. The formation of arsenic-incorporated natroalunites has been also proposed to stabilize the complex arsenic-containing wastes of the nonferrous metal industry [16].

However, the forming conditions of arsenic-incorporated natroalunites within a broad pH range have not been thoroughly examined, and few basic works on the isomorphous replacement have been made [30]. In this paper, pure crystalline natroalunite and pure crystalline arsenic-incorporated natroalunite (As-natroalunite) were synthesized by a simple hydrothermal technique and then characterized using several instruments to investigate the influences of the arsenic incorporation on the structure and morphology of the arsenic-incorporated natroalunite. The dissolution mechanisms of the synthetic natroalunite and the arsenic-incorporated natroalunite were studied at different temperatures and initial pHs. Moreover, the total solution concentrations of sodium, aluminum, sulfate, and arsenate from the dissolution experiments were applied to calculate their solubility product and Gibbs free energy of formation.

2. Experimental Methods

2.1. Solid Preparation and Characterization

2.1.1. Solid Preparation. The arsenic-free natroalunite was hydrothermally prepared after the following reaction with the stoichiometric $Na:Al:SO_4$ mole ratio of $1:3:2$: $Na^+ + 3Al^{3+} + 2SO_4^{2-} + 6OH^- = NaAl_3(SO_4)_2(OH)_6$ [7]. The arsenic-incorporated natroalunite was prepared with a Na^+ excess because of the adding of NaOH to adjust solution pH, and aluminum was therefore the controlling constituent in the synthesis of the arsenic-incorporated natroalunite. Firstly, a Na + Al precursor solution was prepared by dissolving 35.9872 g of $Al_2(SO_4)_3{\cdot}18H_2O$ and 2.5567 g of Na_2SO_4 in 50 mL pure water with stirring at 600 r/min for 30 min. 150 mL pure water or the mixture of 20 mL of 1 M H_3AsO_4 solution and 130 mL pure water were then added into the Na + Al solution. After this, the resulting mixing slurries were regulated to pH 4.00 with 1M NaOH solution, quickly agitated for 30 min, and finally heated at 200°C for 2~48 h in 200 mL stainless-steel autoclaves. After cooling, the obtained products were filtered, washed three times with pure water, and dried at 110°C for 24 h.

2.1.2. Characterization. The solid chemical components were determined by dissolving 0.05 g of the synthetic arsenic-free natroalunite or the synthetic arsenic-incorporated natroalunite in 20 mL of 6 mol/L chlorhydric acid and then diluted in 50 mL volumetric flasks with ultrapure water. The total concentrations of sodium, aluminum, arsenic, and sulfur were analyzed using an inductively coupled plasma-optical emission spectrometer (ICP-OES, PerkinElmer Optima 7000 DV). Assuming the structure of S + As = 2, the formula coefficients for the synthetic solids were then calculated. All synthetic natroalunites before and after the dissolution experiment were investigated by an X-ray diffractometer (XRD, X'Pert PRO) operated at 40 kV and 40 mA with Cu Kα radiation over the scanning 2θ range of 10°~90° at the interval of 0.10°/minute. Besides, the solids

were characterized using a Fourier-transform infrared spectrophotometer (FT-IR, Nicolet Nexus 470) over 4000~400 cm^{-1} in the KBr pellet. The solid morphologies were examined under a field-emission scanning electron microscope (FE-SEM, Hitachi S-4800).

2.2. Dissolution Experiment. For each of the dissolution experiments, four grams of the synthetic natroalunite or the synthetic arsenic-incorporated natroalunite was weighed and then put in 100 mL polypropylene bottle. And afterwards, 100 mL of nitric acid solution (pH 2.00/4.00) or pure water (pH 5.60) was filled. All bottles were capped and placed in three water baths of different temperatures (25°C, 35°C, and 45°C). The mixed solid solutions were stirred using magnetic stirrers. Their pHs were allowed drifting freely and monitored by measurement at regular time. During the dissolution experiments, the aqueous solutions (5 mL) were collected from each bottle at 22 time intervals (1 h, 3 h, 6 h, 12 h, 1 d, 2 d, 5 d, 10 d, 15 d, 20 d, 30 d, 45 d, 60 d, 75 d, 90 d, 120 d, 150 d, 180 d, 210 d, 240 d, and 300 d), filtered into the 25 mL volumetric flask using 0.22 μm disposable syringe filter and immediately acidified with 0.2% nitric acid solution before storing them refrigerated for analysis. 5 mL of the acidic solution or ultrapure water was supplemented after each solution sampling and their dilution effects were taken into account in the PHREEQC calculation. The total dissolved concentrations of sodium, aluminum, arsenic, and sulfur were also determined using the PerkinElmer ICP-OES instrument. The total dissolved concentrations of sulfur and arsenic were given below as sulfate and arsenate since they are the dominating species under the dissolution condition. The dissolution tests of the samples at 25°C and initial solution pH 2.00 were performed in duplicate to check the reproducibility of the results.

2.3. Thermodynamic Calculation. Speciation-solubility calculation was carried out with the pHs, the temperatures, and the total dissolved concentrations of sodium, aluminum, arsenic, and sulfur from the batch dissolutions. The aqueous activities of Na^+, Al^{3+}, AsO_4^{3-}, SO_4^{2-}, and OH^- were calculated using PHREEQC with its minteq.v4.dat database, and the solubility product (K_{sp}) was computed in terms of the mass-action expression of the stoichiometric dissolution. The minteq.v4.dat database includes all thermodynamic data from the MINTEQA2 database file [31–33]. The Debye–Hückel equations were applied in the PHREEQC calculation since all solution ionic strengths in the present experiment were lower than 0.023 mol/L.

3. Results and Discussion

3.1. Solid Characterization

3.1.1. Chemical Composition. The formula coefficients for the synthetic natroalunite and the synthetic arsenic-incorporated natroalunite were estimated from the ICP chemical analysis to be $Na_{0.93}(H_3O)_{0.61}Al_{2.82}(SO_4)_2(OH)_6$ and $Na_{0.88}(H_3O)_{2.44}Al_{2.35}(AsO_4)_{0.38}(SO_4)_{1.62}(OH)_6$, respectively. The precipitates almost always had an apparent Al deficiency in the B^{3+} sites and an appreciable Na deficiency in the A^+ sites (7~12%) of the natroalunite $AB_3(TO_4)_2(OH)_6$. The latter might reflect an incorporation of H_3O^+ to form a solid solution that was hardly proved since H_3O^+ cannot be measured directly using microprobe technique or wet chemistry [34]. Up to 14% of the B^{3+} sites could be unoccupied, which were also probably charge-balanced by H_3O^+ [35]. Hereafter, there might be a large degree of changeability in the natroalunite component, which will in turn influence the solution Na : Al : As : S ratio during dissolution.

3.1.2. X-Ray Diffractometric Analysis. The XRD patterns of the synthetic natroalunite and the arsenic-incorporated natroalunite before and after dissolution are shown in Figure 1. For the natroalunite and the arsenic-incorporated natroalunite prepared, the natroalunite-type mineral was the only phase in comparison with the Reference code 01-089-3952 for natroalunite. The reflection peaks of the synthetic arsenic-incorporated natroalunite shifted gradually to a lower angle with the increase in the AsO_4-for-SO_4 replacement [7]. The cell parameters a and c were determined to be 6.9870 Å and 16.5840 Å for the synthetic natroalunite and 7.0016 Å and 16.7053 Å for the arsenic-incorporated natroalunite, respectively. The cell parameter a of ~7 Å predominantly depends on the B atomic radius and the cell parameter c of ~17 Å on the A and T atomic radius. Due to the significantly greater As-O bond length (~1.57 Å) than the S-O bond length (~1.45 Å) in the TO_4 tetrahedra that is perpendicular to the c axis, the AsO_4-for-SO_4 replacement would enlarge especially the parameter c of natroalunite [36]. Additionally, the A^+ ions in the 12-fold coordination $[AO_6(OH)_6]$ polyhedra that lie between two TO_4-tetrahedra layers can strongly influence the interlayer spacing in the natroalunite crystals. Thus, when significant H_3O^+ substitution happened together with the AsO_4-for-SO_4 substitution in the crystal lattice, both substitution effects overlapped [28, 30, 36].

3.1.3. Fourier-Transform Infrared Spectra Analysis. The M-O stretching vibration, the AsO_4 vibration, the SO_4 vibration, and the OH bending/stretching vibration could be identified in the FT-IR spectra for the natroalunite and the arsenic-incorporated natroalunite before and after dissolution (Figure 2). The stretching vibration bands of the AlO_6 octahedra were found to be around 513~515 and ~480 cm^{-1} [24, 30, 37, 38]. The 1026~1030 cm^{-1} bands, the 426~434 cm^{-1} bands, the ~1207 and ~1099 cm^{-1} bands, and the 663~665 and 627~631 cm^{-1} bands were assigned to the $\nu_1(SO_4)$ symmetric stretching vibration, the $\nu_2(SO_4)$ symmetric stretching vibration, the $\nu_3(SO_4)$ antisymmetric stretching vibration, and the $\nu_4(SO_4)$ vibration, respectively [24, 30]. The 604 cm^{-1} bands and the 3452~3460 cm^{-1} bands belonged to the OH^- bending vibration and the OH^- stretching vibration, respectively [24, 30]. The 1637~1639 cm^{-1} vibration bands were attributed to the framework deformation of powerful H-bonded H_2O molecule [30, 37]. Additionally, the

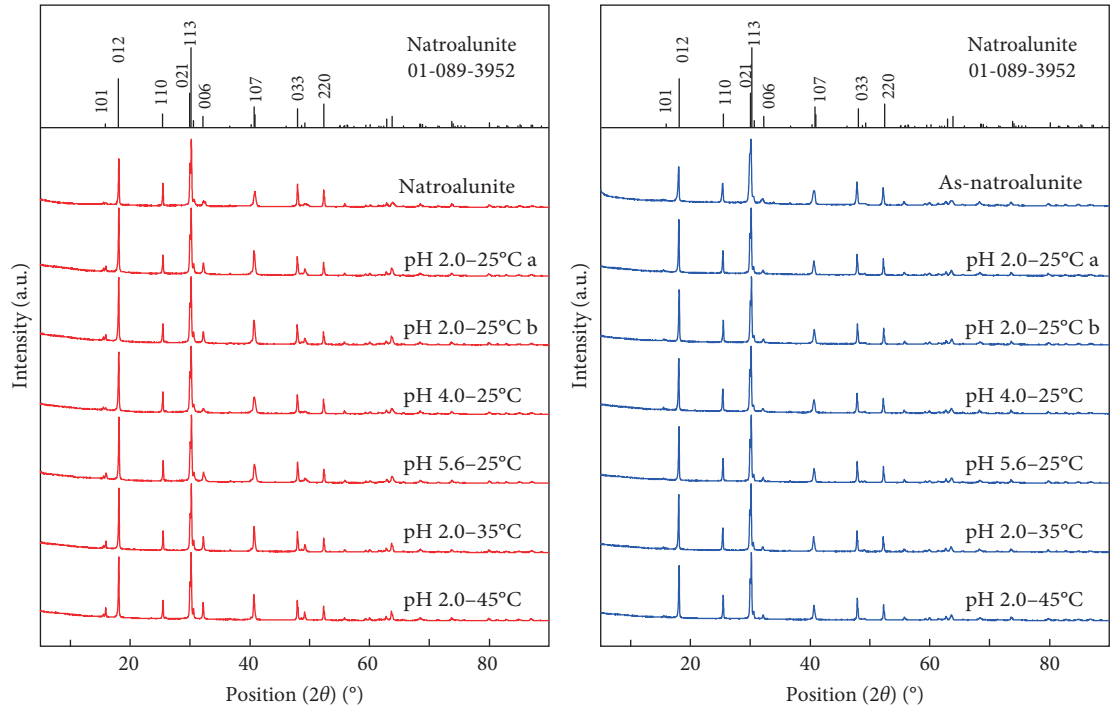

Figure 1: X-ray diffraction patterns of the synthetic natroalunite and the synthetic arsenic-incorporated natroalunite before and after dissolution at 25–45°C for 300 d.

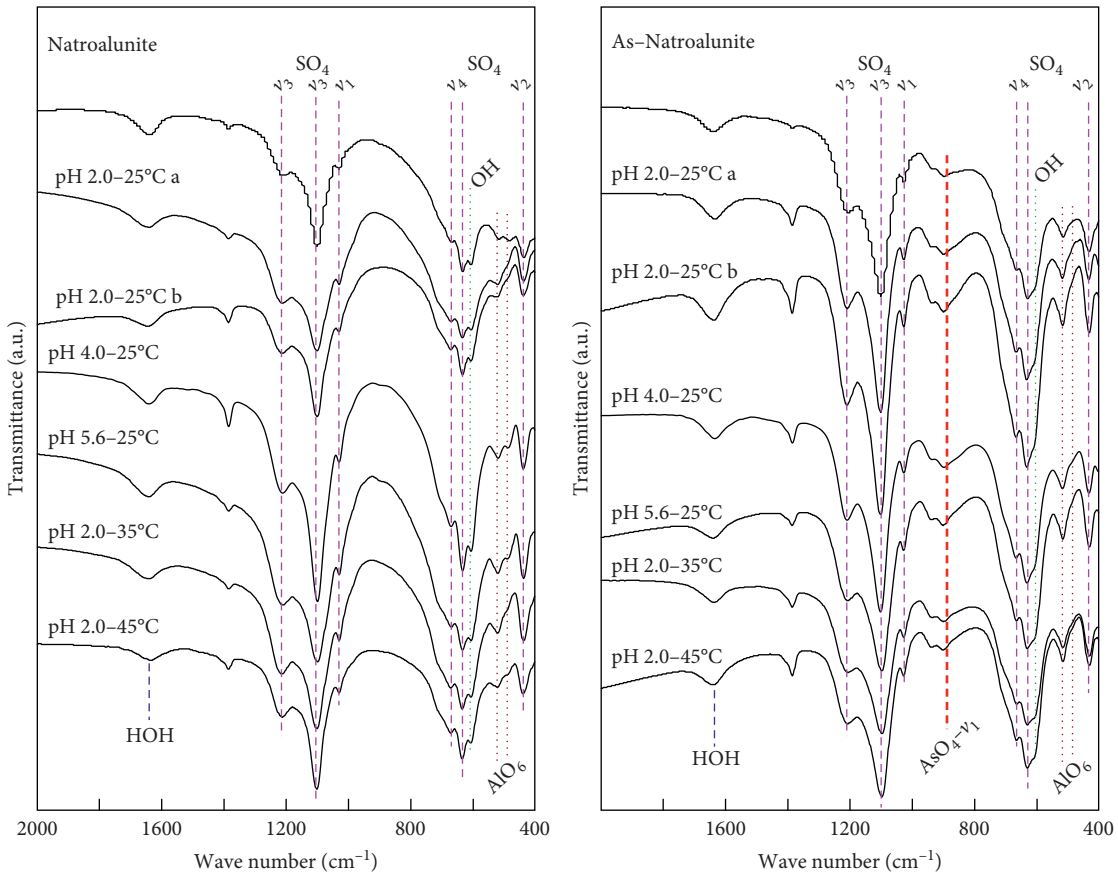

Figure 2: Fourier-transform infrared spectra of the synthetic natroalunite and the synthetic arsenic-incorporated natroalunite before and after dissolution at 25–45°C for 300 d.

symmetric stretching vibration $\nu_1(AsO_4)$ around 895 cm^{-1} was recognized for the arsenic-incorporated natroalunite.

3.1.4. Scanning Electron Micrograph Analysis. The morphology of the synthetic natroalunite and the arsenic-incorporated natroalunite before and after dissolution at initial pH 2.00 and 25°C is illustrated in Figure 3. The precipitates showed pseudo-octahedral crystal forms (2~5 μm size) with certain nanosized fine grains, which were also approved to be the natroalunite phase by ICP and XRD analyses. The arsenate-for-sulfate substitution did not change the morphologies of the natroalunite crystals, i.e., the pseudo-octahedra (regular ditrigonal scalenohedra), which looked like spheroid due to the probable precipitation-dissolution process. The trigonal crystals of natroalunite are morphologically rhombohedra with a 90°50′ interfacial angle, which makes them look like cubes [28, 30] or the ditrigonal scalenohedral looks like octahedra in the present work (Figure 3). Nevertheless, even in the case of the extreme dissolution at initial pH 2.00 and 25°C what appeared to be the original crystal boundaries remained well-preserved.

3.2. Evolution of Solution pH and the Total Elemental Concentrations during Dissolution. The total dissolved concentrations of sodium, aluminum, arsenic, and sulfur and their mole ratios for the dissolution of the arsenic-free and arsenic-incorporated natroalunites at different initial pHs and temperatures are plotted versus the long-term dissolution time in Figures 4 and 5.

For the dissolution of the synthetic natroalunite and the synthetic arsenic-incorporated natroalunite at initial pH 2.00 and 25°C (Figures 4 and 5), the solution pHs increased from 2.00 to 4.10 and from 2.00 to 4.00 within 120 h of dissolution and then varied between 3.96~4.34 and 3.93~4.22, respectively. For the dissolution at initial pH 4.00 and 25°C, the solution pHs increased from 4.00 to 4.61~5.47 within the first 3 h of interaction and then decreased gradually and finally varied between 4.14~4.43 after 48 h. For the dissolution at initial pH 5.60 and 25°C, the solution pHs decreased from 5.60 to 4.55 and from 5.60 to 5.13 within 24~72 h of dissolution and then varied between 4.33~4.68 and 4.62~5.21, respectively. It is consistent with the results that the solution pHs declined to pH ~3.8 for the dissolution of jarosite in the water of pH 4, while in its dissolution at pH 3, the solution pHs rose to about 3.2, which means that jarosite and its dissolution resultants had certain pH buffering capability [25]. Various dissolution mechanisms dominated at high and low pHs, i.e., jarosite dissolution could either increase the pHs of aqueous acidic mediums (initial pHs <3~4) or decrease the pHs of aqueous subneutral-alkaline mediums due to the H^+ depleting as the dissolution reactions proceeded [39]. Two different dissolution mechanisms for jarosite occurred at low (<3.5) and high (>3.5) pHs. Under low pH (<3.5) condition, the solution pHs increased gradually with time, suggesting H^+ depleting [40]. This result indicated that the jarosite dissolution at pH <3.5 followed the mechanism that consumed H^+ and produced aqueous Fe^{3+} species. Particularly in the low pH solution with H_2SO_4, aqueous Fe^{3+}-SO_4^{2-} complexes would control the aqueous Fe^{3+} speciation. On the contrary, under high pH (>3.5) condition, the solution pHs declined with time, indicating a OH^- consumption in the dissolution [40].

The dissolved Na^+ concentrations rose quickly at the start and attained the highest values after about 240 h of dissolution. A steady state was approached after 2160 h of interaction. The AsO_4-for-SO_4 replacement had a great influence on the Na^+ release, i.e., the dissolved Na^+ concentrations increased significantly with the increase of this substitution. The increase of the initial solution pH was not beneficial for the Na^+ release into solution. The temperature showed also an obvious influence on the Na^+ release. For the dissolution of the synthetic natroalunite, the Na^+ release rates increased in the following order: 25°C > 45°C > 35°C. For the dissolution of the synthetic arsenic-incorporated natroalunite, the Na^+ release rates increased in the following order: 35°C > 45°C > 25°C.

The dissolved Al^{3+} concentrations rose quickly at the start and attained the highest values after about 12 h of dissolution and then declined slowly. After 2160 h of interaction, a steady status was approached. The AsO_4-for-SO_4 replacement had a great influence on the Al^{3+} release. On the contrary to the Na^+ release, the dissolved Al^{3+} concentrations decreased significantly with the increase of this substitution. The increase of the initial solution pH could obviously decrease the Al^{3+} release into solution. The temperature showed also an obvious influence on the Al^{3+} release. For the dissolution of the synthetic natroalunite, the Al^{3+} release rates increased in the following order: 25°C > 35°C > 45°C. For the dissolution of the synthetic arsenic-incorporated natroalunite, the Al^{3+} release rates increased in the following order: 35°C > 45°C > 25°C.

The dissolved SO_4^{2-} concentrations generally fluctuated within the first 2880 of the reaction and then gradually reached a steady state. The dissolved SO_4^{2-} concentrations increased significantly with the increase of the AsO_4-for-SO_4 replacement. For the dissolution of the synthetic natroalunite, the dissolved SO_4^{2-} concentrations rose quickly at the start and attained the highest values after about 480–1800 h of dissolution and then a steady state was gradually approached. The increase of the initial solution pH was not beneficial for the SO_4^{2-} release into solution. The SO_4^{2-} release rates increased in the following order: pH 2.00 > pH 4.00 > pH 5.60 and 25°C ≈ 35°C > 45°C. For the dissolution of the synthetic arsenic-incorporated natroalunite, the SO_4^{2-} release rates increased in the following order: pH 4.00 > pH 2.00 > pH 5.60 and 25°C > 35°C~45°C.

The dissolved AsO_4^{3-} concentrations increased significantly with the increase of the AsO_4-for-SO_4 replacement. For the dissolution of the arsenic-incorporated natroalunite at initial pH 2.00, the dissolved AsO_4^{3-} concentrations rose quickly at the start and attained the highest values after about 6–24 h of dissolution. After that, the dissolved AsO_4^{3-} concentrations decreased gradually and a steady state was gradually approached after 2880 h of dissolution. The temperature increase was beneficial for the AsO_4^{3-} release into solution. The dissolved AsO_4^{3-} concentrations for the

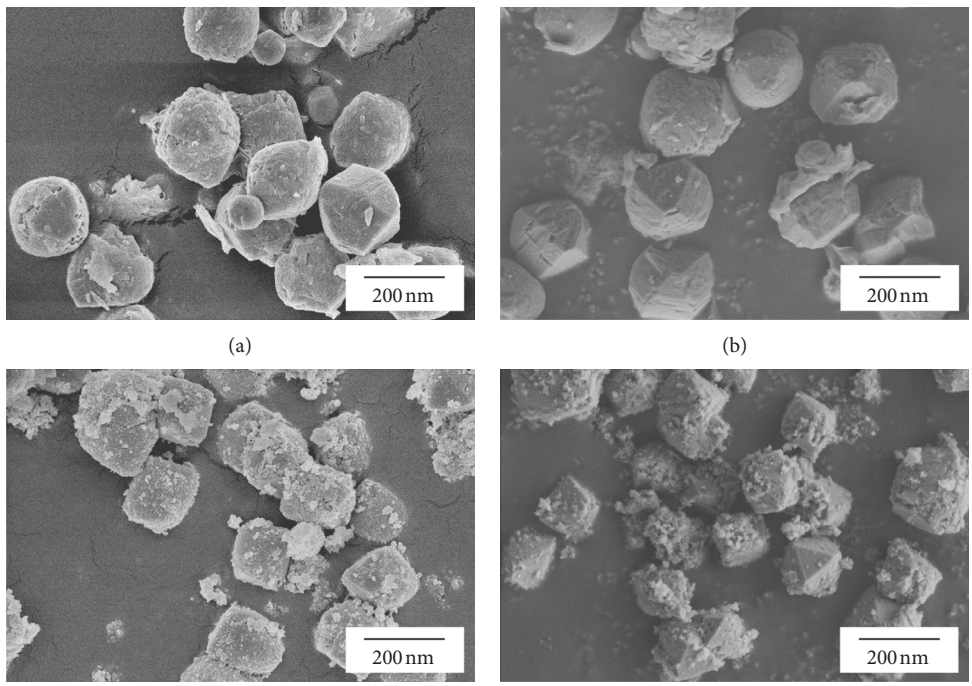

Figure 3: Field-emission scanning electron microscopic images of the synthetic natroalunite and the synthetic arsenic-incorporated natroalunite before and after dissolution at 25°C for 300 d.

dissolution at 35°C and 45°C were slightly greater than those at 25°C. For the dissolution at the initial pHs of 4.00 and 5.60, the dissolved AsO_4^{3-} concentrations increased gradually in the first 720 h and then approached to a steady state.

3.3. Overall Dissolution Reaction and Mechanism. The solution pHs were always greater than 2.00 for the dissolution at initial pH 2.00. The hydrion depleting indicated that the H^+ sorption onto negatively charged oxygen ions of the arsenate and sulfate groups of (As-)natroalunite might result in the conversion of AsO_4^{3-} and SO_4^{2-} to $H_2AsO_4^-$ and HSO_4^- on the natroalunite surface and accelerate the dissolution process. Furthermore, the dissolution/exchange coexistence suggested that the hydrion depleting was caused not only by the hydrion adsorption/desorption but by many different reactions on the (As-)natroalunite surface [7]. Therefore, a comprehensive elucidation of the hydrion depleting should include at least the stoichiometric dissolution of (As-)natroalunite and the speciation of dissolved components in solution.

3.3.1. Natroalunite $[Na_{0.93}(H_3O)_{0.61}Al_{2.82}(SO_4)_2(OH)_6]$. Dissolution in the present experiment did not result in the formation of any measurable precipitates based on the XRD and FE-SEM results (Figures 1 and 3), which was in accordance with the saturation index calculation with PHREEQC. The stoichiometric dissolution reaction of the synthetic natroalunite $[Na_{0.93}(H_3O)_{0.61}Al_{2.82}(SO_4)_2(OH)_6]$ could be simply expressed by the following dissolution equation:

$$\begin{aligned} &Na_{0.93}(H_3O)_{0.61}Al_{2.82}(SO_4)_2(OH)_6 \\ &\quad = 0.93\,Na^+ + 0.61\,H_3O^+ + 2.82\,Al^{3+} + 2\,SO_4^{2-} + 6\,OH^- \\ &\quad = 0.93\,Na^+ + 2.82\,Al^{3+} + 2\,SO_4^{2-} + 5.39\,OH^- + 1.22\,H_2O \end{aligned} \quad (1)$$

The reaction could produce 5.39 mol OH^- for a mole of dissolved natroalunite. Thus, the natroalunite dissolution at lower initial pH could result in a pH increase, suggesting hydrion depleting or OH^- releasing. This indicated that the natroalunite dissolution at lower pHs followed a reaction mechanism which consumed hydrions and the Al/sulfate complexes should dominate the aqueous speciation of Al^{3+}:

$$Al^{3+} + nOH^- = Al(OH)_n^{(3-n)+}, \quad n = 1\sim4 \quad (2)$$

$$H^+ + SO_4^{2-} = HSO_4^- \quad (3)$$

For the dissolution of the synthetic natroalunite $[Na_{0.93}(H_3O)_{0.61}Al_{2.82}(SO_4)_2(OH)_6]$ at 25°C and initial pH 2.00 (Figure 4), the dissolved Na^+, Al^{3+}, and SO_4^{2-} concentrations rose quickly and simultaneously in the first 0–3 h of interaction with the aqueous Na/Al mole ratios of 0.30–0.34, the aqueous Al/SO_4 mole ratios of 1.44–1.59, and the aqueous Na/SO_4 mole ratios of 0.54–0.71, which were in close proximity to the stoichiometric Na/Al, Al/SO_4, and Na/SO_4 mole ratios of 0.33, 1.41, and 0.47 for the synthetic natroalunite, respectively. This result is similar to the observation in the dissolution experiments of alunite [20], arsenojarosite [41], Na-jarosite [19, 39], and K-jarosite [21, 40], i.e., nearly congruent dissolutions were observed at

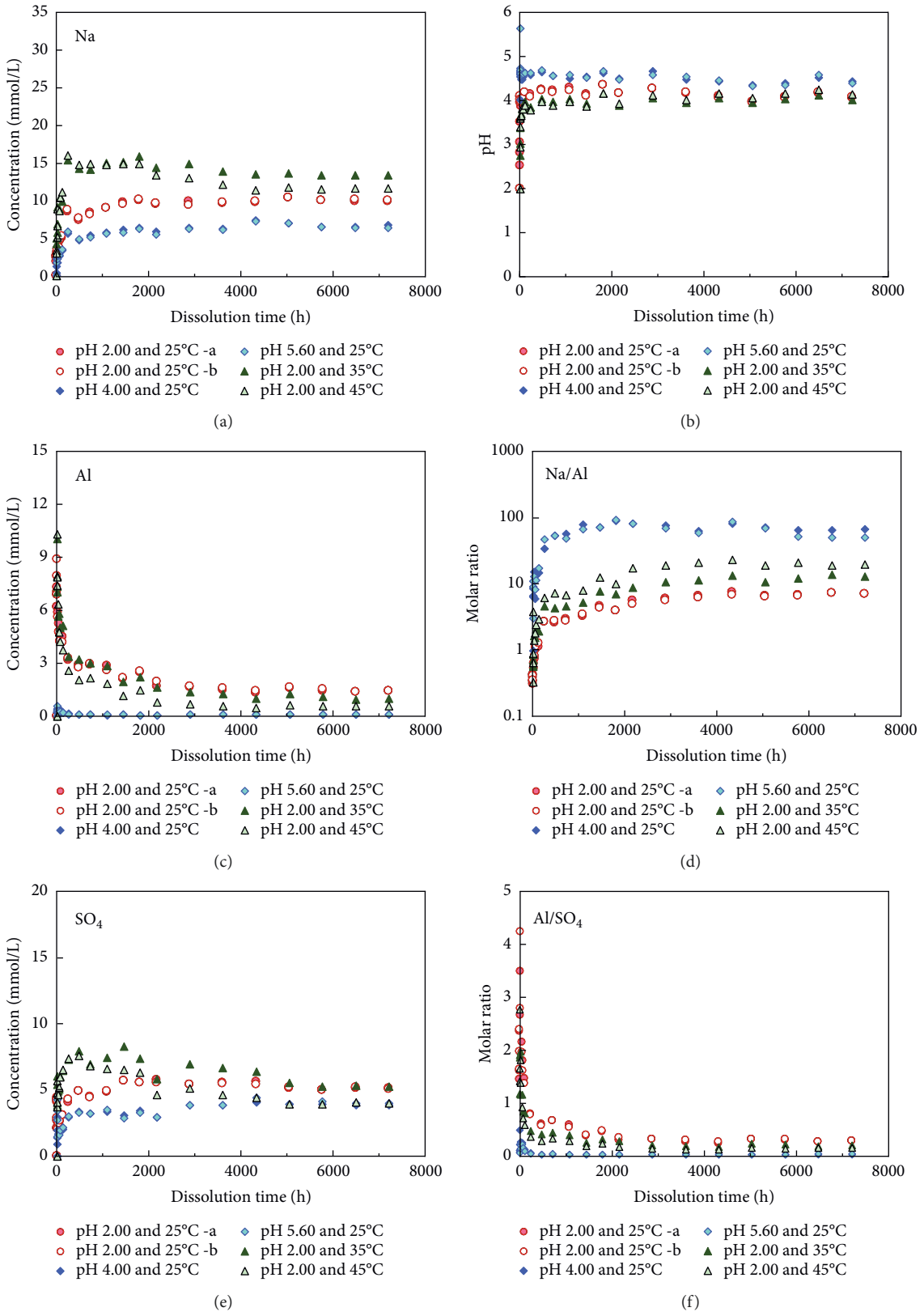

Figure 4: Aqueous evolution during the dissolution of the synthetic natroalunite at 25–45°C for 300 d.

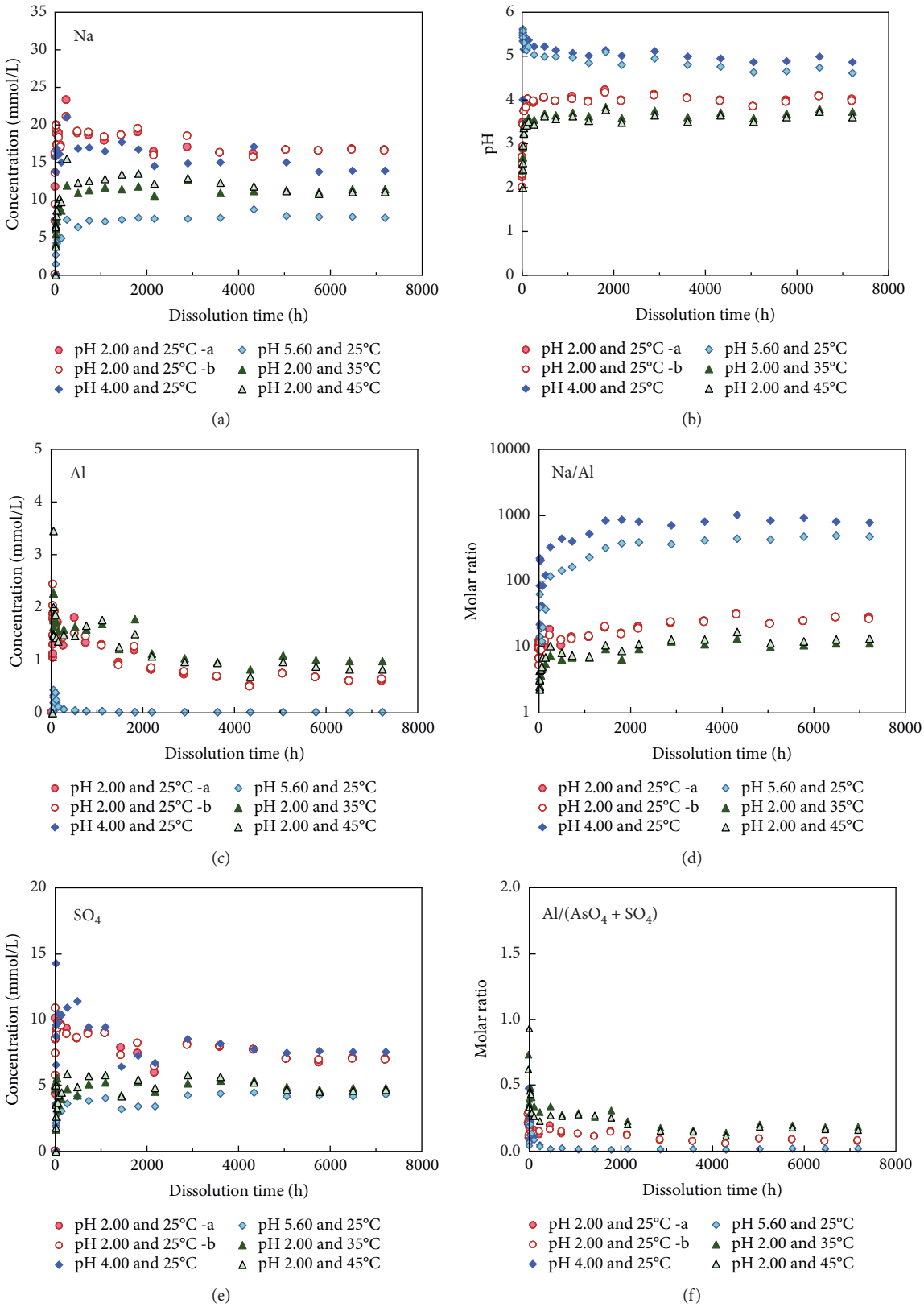

Figure 5: Continued.

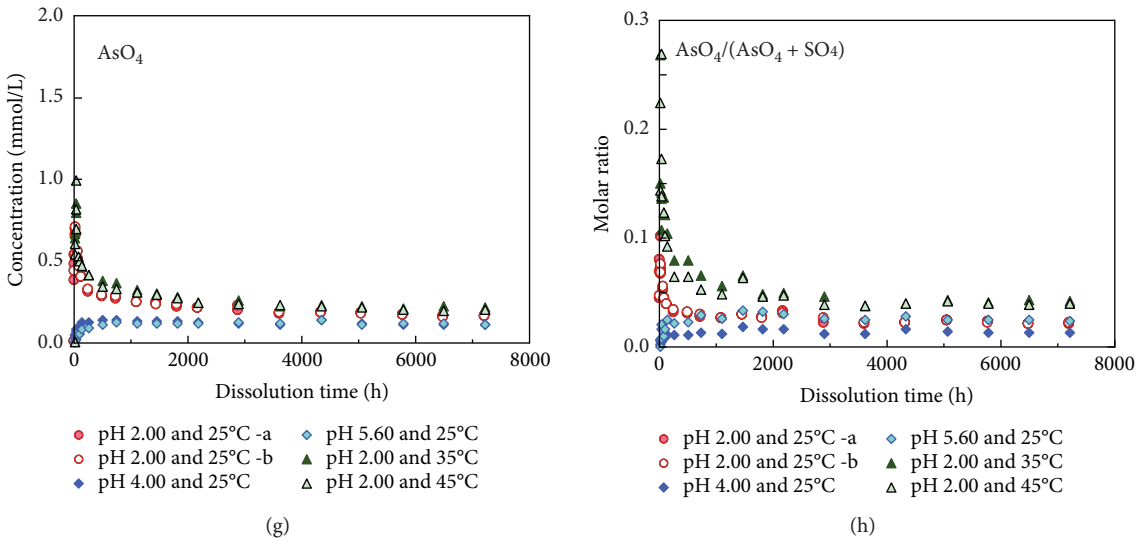

Figure 5: Aqueous evolution during the dissolution of the synthetic arsenic-incorporated natroalunite at 25–45°C for 300 d.

low pHs, whereas incongruent dissolutions were found at circum-neutral to high pHs. Two different dissolution mechanisms, one for lower pHs and the other for higher pHs, might take place [42].

A shift from congruent to incongruent dissolution could be observed over the longer term [19]. As the time increased, the synthetic natroalunite dissolved nonstoichiometrically and released Na^+ preferentially over Al^{3+} to the aqueous solution, and the aqueous Na/Al and Na/SO_4 mole ratios increased and the aqueous Al/SO_4 mole ratios decreased rapidly. After 3 h, the aqueous Na^+ and Al^{3+} concentrations as well as the solution pHs increased continuously, while the total aqueous SO_4^{2-} concentrations decreased rapidly. From 12 h to 2880 h, the pHs approached a steady state (3.96~4.34), the aqueous Na^+ and SO_4^{2-} concentrations increased, while the aqueous Al^{3+} concentrations decreased slowly. The cations in the A sites could be preferentially released to solution at the start of dissolution, while the cations in the B sites would be preferentially retained in solid [19]. Alunite dissolved almost congruently for the experiment at pH around 3 (i.e., dissolved Al/K mole ratio ≈3) or incongruently for the experiment at pH ≥ 3.9 (i.e., dissolved Al/K mole ratio <3) [42].

After 2880 h of dissolution, the solution pHs and the total solution Na^+, Al^{3+}, and SO_4^{2-} concentrations tending to reach the steady state with the stoichiometric Na/Al, Al/SO_4, and Na/SO_4 mole ratios were around 6.54–7.35, 0.24–0.29, and 1.74–2.03, which were significantly higher than the stoichiometric Na/Al, Al/SO_4, and Na/SO_4 mole ratios of 0.33, 1.41, and 0.47 for the synthetic natroalunite, respectively (Figure 4). This means that Na^+ cations preferred to be released from solid to solution relative to Al^{3+} and SO_4^{2-} ions and the SO_4^{2-} anions preferred to be released from solid to solution relative to Al^{3+} ions, i.e., the components were released from solid to solution preferentially after the following order: Na^+ $(H_3O^+) > SO_4^{2-} > Al^{3+}$. Additionally, this differential tendency became more obvious with the increasing dissolution temperature and initial solution pHs. Selective release of Na^+ in the A site and SO_4^{2-} in the T site resulted in higher aqueous Na^+ and SO_4^{2-} concentrations compared to Al^{3+} deep in the T-O-T structure of natroalunite [21]. Similar selective release of K^+ and SO_4^{2-} was also reported for the jarosite dissolution [21, 43]. Jarosite dissolved near-congruently in the first few days and then incongruently with a decrease of the dissolved Fe^{3+} concentration and an increase of the dissolved SO_4^{2-} concentration, which would result in the formation of an Fe-rich residuum [19].

The speciation calculation using PHREEQC showed that for the natroalunite dissolution at initial pH 2.00 and 25°C, the aluminum species appeared in the sequence of $AlSO_4^+ > Al^{3+} > Al(SO_4)_2^- > Al(OH)^{2+} > Al(OH)_2^+ > AlHSO_4^{2+} > Al(OH)_3^0 > Al(OH)_4^-$; the sulfate species appeared in the sequence of $SO_4^{2-} > AlSO_4^+ > NaSO_4^- > Al(SO_4)_2^- > HSO_4^- > AlHSO_4^{2+}$. The concentrations of all sodium, aluminum, and sulfate species attained a steady state at the experimental end.

3.3.2. As-Natroalunite $[Na_{0.88}(H_3O)_{2.44}Al_{2.35}(AsO_4)_{0.38}(SO_4)_{1.62}(OH)_6]$. The stoichiometry of the synthetic As-natroalunite dissolution reaction varied as a function of time, solution pH, and temperature. The speciation of dissolved Al^{3+}, AsO_4^{3-}, and SO_4^{2-} can strongly affect the pH-dependence of the dissolution stoichiometry [19]. The stoichiometric dissolution of the synthetic arsenic-incorporated natroalunite $[Na_{0.88}(H_3O)_{2.44}Al_{2.35}(AsO_4)_{0.38}(SO_4)_{1.62}(OH)_6]$ can be expressed by the general reaction as follows:

$$\begin{aligned} Na_{0.88}(H_3O)_{2.44}Al_{2.35}(AsO_4)_{0.38}(SO_4)_{1.62}(OH)_6 \\ = 0.88\,Na^+ + 2.44\,H_3O^+ + 2.35\,Al^{3+} + 0.38\,AsO_4^{3-} \\ + 1.62\,SO_4^{2-} + 6\,OH^- \\ = 0.88\,Na^+ + 2.35\,Al^{3+} + 0.38\,AsO_4^{3-} + 1.62\,SO_4^{2-} \\ + 3.56\,OH^- + 4.88\,H_2O \end{aligned} \quad (4)$$

Theoretically, one mole of the arsenic-incorporated natroalunite would release 3.56 mol OH^- according to this dissolution reaction. Consequently, its dissolution at lower initial pH could result in a pH increase with time, suggesting OH^- release or H^+ depletion. The As-natroalunite dissolution at lower pHs followed the reaction mechanisms that consumed H^+ ions, and the aqueous Al/sulfate/arsenate complexes should dominate the aqueous speciation of Al^{3+} (equations (2), (3), and (5)).

$$nH^+ + AsO_4^{3-} = H_nAsO_4^{(3-n)-}, \quad n = 1\sim3 \tag{5}$$

For the dissolution of the synthetic As-natroalunite $[Na_{0.88}(H_3O)_{2.44}Al_{2.35}(AsO_4)_{0.38}(SO_4)_{1.62}(OH)_6]$ at 25°C and initial pH 2.00 (Figure 5), the solution Na/Al mole ratios reached 6.84–5.21 in the first hour dissolution and then increased gradually with time; the aqueous $AsO_4/(AsO_4 + SO_4)$ mole ratios increased with time and reached 0.08–0.10 in 6–12 h dissolution and then decreased gradually with time; the aqueous $Na/(AsO_4 + SO_4)$ mole ratios fluctuated greatly within 5040 h dissolution; the aqueous $Al/(AsO_4 + SO_4)$ mole ratios decreased generally with time.

The transient peak values in the total dissolved Na^+, Al^{3+}, AsO_4^{3-}, and SO_4^{2-} concentrations during the mineral dissolution between 3 and 240 h were also reported in earlier researches, which was possibly related to the particle size dispersion [19, 44]. The smaller the particle size of the As-natroalunite, the larger its dissolution rate and solubility. Henceforth, the transient highest concentrations might result from the faster dissolution of finer particles and the following reprecipitation to coarser particles [44].

After 5760 h of dissolution, the solution pHs and the total dissolved Na^+, Al^{3+}, AsO_4^{3-}, and SO_4^{2-} concentrations became constant and reached the steady state with the stoichiometric Na/Al, and $Na/(AsO_4 + SO_4)$ mole ratios were around 24.73–28.08 and 2.29–2.39, which were significantly higher than the stoichiometric Na/Al and $Na/(AsO_4 + SO_4)$ mole ratios of 0.37 and 0.44 for the synthetic As-natroalunite, and the stoichiometric $AsO_4/(AsO_4 + SO_4)$ and $Al/(AsO_4 + SO_4)$ mole ratios were around 0.02 and 0.08–0.10, which were significantly lower than the stoichiometric $AsO_4/(AsO_4 + SO_4)$ and $Al/(AsO_4 + SO_4)$ mole ratios of 0.16 and 1.18 for the synthetic As-natroalunite, respectively (Figure 5). This means that Na^+ cations preferred to be released from solid to solution relative to Al^{3+}, AsO_4^{3-}, and SO_4^{2-} ions, the SO_4^{2-} anions preferred to be released from solid to solution relative to AsO_4^{3-} anions, and the AsO_4^{3-} and SO_4^{2-} anions preferred to be released from solid to solution relative to Al^{3+} cations, i.e., the components were released from solid to solution preferentially after the following order: Na^+ $(H_3O^+) > SO_4^{2-} > AsO_4^{3-} > Al^{3+}$, suggesting incongruent dissolution of the (As-)natroalunite and/or formation of AsO_4/Al-rich residuals as the alunite dissolution at pH > 5 [20].

K-Cr(VI)-jarosites dissolved congruently in acidic solutions and incongruently in alkaline solutions [45]. The dissolution rate was properly limited by the release of both B or TO_4 groups from natroalunite, which would be hindered by the outer Na^+ and OH^- group layers that were energetically stable in the solvated surface [42]. The dissolution was restrained by the Al–O bond breakage in the $AB_3(TO_4)_2(OH)_6$ structure of the alunite supergroup [40, 45]. Al^{3+} ions were left behind either as a reprecipitated Al-rich phase or as a residue of the alunite octahedral layers in the solid phase [25]. The degree of replacement of other ions into the $AB_3(TO_4)_2(OH)_6$ structure can affect the stability and reactivity of the alunite supergroup minerals [25].

Additionally, this differential tendency became more obvious with the increasing dissolution temperature and initial solution pHs. For the dissolution of the synthetic As-natroalunite $[Na_{0.88}(H_3O)_{2.44}Al_{2.35}(AsO_4)_{0.38}(SO_4)_{1.62}(OH)_6]$ at 25°C and initial pH 4.00/5.60 (Figure 5), the solution Na/Al mole ratios were significantly higher and the $Na/(AsO_4 + SO_4)$, $Al/(AsO_4 + SO_4)$ and $AsO_4/(AsO_4 + SO_4)$ mole ratios were lower than the values for their dissolution at initial pH 2.00. For the dissolution of the synthetic As-natroalunite $[Na_{0.88}(H_3O)_{2.44}Al_{2.35}(AsO_4)_{0.38}(SO_4)_{1.62}(OH)_6]$ at 35°C/45°C and initial pH 2.00 (Figure 5), the aqueous Na/Al and $Na/(AsO_4 + SO_4)$ mole ratios were lower and the $Al/(AsO_4 + SO_4)$ and $AsO_4/(AsO_4 + SO_4)$ mole ratios were higher than the values for their dissolution at 25°C, which was similar to the experimental result of the K-Cr(VI)-jarosite dissolution [45]. All the performed dissolutions undertook a pH variation that was related to the great H_3O^+/OH^- depleting, extraordinary at the experimental start, i.e., within the short induction period, which was reflected in a drastic pH increase/decrease [45]. The arsenic substitution into jarosite can limit the ability of the OH^- attachment onto the gain surfaces and cause a H_2O attach, which could be related to the electrostatic repulsion of the OH^- ions at higher pH owing to the AsO_4 bonds on the surface; moreover, the increase in the Fe-AsO_4 bond number can inhibit the systems' dependency on H_3O^+/OH^- [41]. This phenomenon was not found in the K-Cr-jarosite dissolution, suggesting an incessant dependency of the reaction on the H_3O^+/OH^-concentration [45].

The speciation calculation using PHREEQC showed that for the As-natroalunite dissolution at initial pH 2.00 and 25°C, the sodium species appeared according to the sequence of $Na^+ > NaSO_4^- > NaH_2AsO_4^0 > NaHAsO_4^- > NaAsO_4^{2-}$; the aluminum species appeared according to the order of $AlSO_4^+ > Al^{3+} > Al(SO_4)_2^- > Al(OH)^{2+} > Al(OH)_2^+ > AlHSO_4^{2+} > AlH_2AsO_4^{2+} > Al(OH)_3^0 > Al(OH)_4^- > AlHAsO_4^+ > AlAsO_4^0$; the arsenate species appeared according to the order of $H_2AsO_4^- > NaH_2AsO_4^0 > H_3AsO_4^0 > HAsO_4^{2-} > AlH_2AsO_4^{2+} > NaHAsO_4^- > NaAsO_4^{2-} > AlHAsO_4^+ > AsO_4^{3-} > AlAsO_4^0$; the sulfate species appeared according to the order of $SO_4^{2-} > AlSO_4^+ > NaSO_4^- > HSO_4^- > Al(SO_4)_2^- > AlHSO_4^{2+}$. At the dissolution start, the concentrations of all sodium, aluminum, arsenate, and sulfate species except HSO_4^- and $AlHSO_4^{2+}$ increased with the dissolution time and finally attained a steady state. The dissolved sodium and sulfate were principally present as Na^+ and SO_4^{2-} within the entire pH range, correspondingly. Nevertheless, the speciation of dissolved aluminum and arsenate displayed an obvious variation with pHs.

For the dissolution of the synthetic natroalunite and the synthetic As-natroalunite at 25°C and initial pH 2.00 (Figures 4 and 5), all solutions were undersaturated with respect to $Al(OH)_3$ from the PHREEQC calculation, i.e., aluminum

(hydr-)oxides were unlikely to precipitate. Instead, it was likely to form some aluminum-rich and arsenic-rich reaction products. Aluminum hydroxides were possibly expected to form only at pH 4.00 and 5.60 because the solutions were oversaturated-saturated with respect to $Al(OH)_3$, although no secondary precipitate on the surface was detected by the XRD and SEM results due to the very small amounts of formation (Figures 1 and 3).

The mechanism for the As-natroalunite dissolution at high pHs shifted from H^+ to OH^- mediated process because of the Al^{3+} hydrolysis [20]. The saturation calculation with PHREEQC for the dissolution at initial pH 2.00 indicated that all solutions were clearly undersaturated as for all possible aluminum (hydr-)oxides (amorphous aluminum hydroxide [$Al(OH)_{3(a)}$], gibbsite [$Al(OH)_3$], diaspore [AlOOH], and $AlAsO_4{\cdot}2H_2O$, $Al_4(OH)_{10}SO_4$), whose precipitation was thermodynamically unfavorable. In contrast, most of the solutions at initial pH 4.00 and 5.60 were nearly saturated with respect to these aluminum (hydr-)oxides, and some precipitation of these phases could not be absolutely ruled out.

3.4. Determination of Solubility. The solubility product (K_{sp}) is equal to the ion activity product (IAP) at the dissolution equilibrium, i.e., the K_{sp} calculation requires that the equilibrium has been attained, which could be simplified using sufficient solid to guarantee that excess (As-)natroalunite remained at equilibrium.

The aqueous activities of Na^+, Al^{3+}, AsO_4^{3-}, SO_4^{2-}, and OH^- in the last three equilibrated solutions (5760 h, 6480 h, and 7200 h) were calculated using PHREEQC with the minteq.v4.dat database [31] to determine the solubility products (K_{sp}) of the synthetic natroalunite and the arsenic-incorporated natroalunite. The solution species Na^+, $NaAsO_4^{2-}$, $NaHAsO_4^-$, and $NaH_2AsO_4^0$ were considered in the simulation for the total sodium; Al^{3+}, $Al(OH)_4^-$, $Al(OH)_3$, $Al(OH)_2^+$, $AlOH^{2+}$, $Al_2(OH)_2^{4+}$, $Al_3(OH)_4^{5+}$, $Al_{13}O_4(OH)_{24}^{7+}$, $AlAsO_4^0$, $AlHAsO_4^+$, $AlH_2AsO_4^{2+}$, $AlHSO_4^{2+}$, $Al(SO_4)_2^-$, and $AlSO_4^+$ for the total aluminum; H_3AsO_4, AsO_4^{3-}, $HAsO_4^{2-}$, $H_2AsO_4^-$, $NaH_2AsO_4^0$, $NaHAsO_4^-$, $NaAsO_4^{2-}$, $AlAsO_4^0$, $AlHAsO_4^+$, and $AlH_2AsO_4^{2+}$ for the total arsenate; SO_4^{2-}, HSO_4^-, $AlHSO_4^{2+}$, $Al(SO_4)_2^-$, and $AlSO_4^+$ for the total sulfate.

The stoichiometrical dissolution reactions of the synthetic natroalunite [$Na_{0.93}(H_3O)_{0.61}Al_{2.82}(SO_4)_2(OH)_6$] and the synthetic arsenic-incorporated natroalunite [$Na_{0.88}(H_3O)_{2.44}Al_{2.35}(AsO_4)_{0.38}(SO_4)_{1.62}(OH)_6$] can be described with the dissolution reactions (1) and (4), respectively.

Presuming unit activity of the solid is as follows:

$$K_{sp} = \{Na^+\}^{0.93}\{Al^{3+}\}^{2.82}\{SO_4^{2-}\}^2\{OH^-\}^{5.39} \quad (6)$$

$$\text{or } K_{sp} = \{Na^+\}^{0.88}\{Al^{3+}\}^{2.35}\{AsO_4^{3-}\}^{0.38}\{SO_4^{2-}\}^{1.62}\{OH^-\}^{3.56} \quad (7)$$

where {} is the thermodynamic activity and K_{sp} is the solubility product according to the dissolution reactions (1) and (4).

The Gibbs free energies of formation, $\Delta G_f^\circ[Na_{0.93}(H_3O)_{0.61}Al_{2.82}(SO_4)_2(OH)_6]$ and $\Delta G_f^\circ[Na_{0.88}(H_3O)_{2.44}Al_{2.35}(AsO_4)_{0.38}(SO_4)_{1.62}(OH)_6]$, can also be estimated by the use of the following thermodynamic data in the literature [46, 47], $\Delta G_f^\circ[Na^+] = -262$ kJ/mol, $\Delta G_f^\circ[Al^{3+}] = -489.4$ kJ/mol, $\Delta G_f^\circ[AsO_4^{3-}] = -647.618$ kJ/mol, $\Delta G_f^\circ[SO_4^{2-}] = -744.6$ kJ/mol, $\Delta G_f^\circ[OH^-] = -157.3$ kJ/mol, and $\Delta G_f^\circ[H_2O] = -237.18$ kJ/mol. The K_{sp} value is related to the standard free energy of reaction (ΔG_r^o) and can be expressed under the standard condition (298.15 K and 0.101 MPa) by

$$\Delta G_r^\circ = -5.708 \log K_{sp}. \quad (8)$$

For (1),

$$\begin{aligned}\Delta G_r^\circ = {} & 0.93\,\Delta G_f^\circ[Na^+] + 2.82\,\Delta G_f^\circ[Al^{3+}] + 2\,\Delta G_f^\circ[SO_4^{2-}] \\ & + 1.22\,\Delta G_f^\circ[H_2O] + 5.39\,\Delta G_f^\circ[OH^-] \\ & - \Delta G_f^\circ[Na_{0.93}(H_3O)_{0.61}Al_{2.82}(SO_4)_2(OH)_6]\end{aligned} \quad (9)$$

Rearranging,

$$\begin{aligned}\Delta G_f^\circ & [Na_{0.93}(H_3O)_{0.61}Al_{2.82}(SO_4)_2(OH)_6] \\ = {} & 0.93\Delta G_f^\circ[Na^+] + 2.82\,\Delta G_f^\circ[Al^{3+}] + 2\Delta G_f^\circ[SO_4^{2-}] \\ & + 1.22\,\Delta G_f^\circ[H_2O] + 5.39\Delta G_f^\circ[OH^-] - \Delta G_r^\circ\end{aligned} \quad (10)$$

For (4),

$$\begin{aligned}\Delta G_r^o = {} & 0.88\,\Delta G_f^\circ[Na^+] + 2.35\,\Delta G_f^\circ[Al^{3+}] \\ & + 0.38\,\Delta G_f^\circ[AsO_4^{3-}] + 1.62\,\Delta G_f^\circ[SO_4^{2-}] \\ & + 4.88\,\Delta G_f^\circ[H_2O] + 3.56\,\Delta G_f^\circ[OH^-] \\ & - \Delta G_f^\circ[Na_{0.88}(H_3O)_{2.44}Al_{2.35}(AsO_4)_{0.38}(SO_4)_{1.62}(OH)_6]\end{aligned} \quad (11)$$

Rearranging,

$$\begin{aligned}\Delta G_f^\circ & [Na_{0.88}(H_3O)_{2.44}Al_{2.35}(AsO_4)_{0.38}(SO_4)_{1.62}(OH)_6] \\ = {} & 0.88\,\Delta G_f^\circ[Na^+] + 2.35\Delta G_f^\circ[Al^{3+}] + 0.38\,\Delta G_f^\circ[AsO_4^{3-}] \\ & + 1.62\Delta G_f^\circ[SO_4^{2-}] + 4.88\Delta G_f^\circ[H_2O] + 3.56\Delta G_f^\circ[OH^-] \\ & - \Delta G_r^\circ\end{aligned} \quad (12)$$

The calculated solubility products together with the total dissolved concentrations of sodium, aluminum, arsenic, and sulfur including solution pHs in the last three equilibrated solutions (5760 h, 6480 h and 7200 h) are given in Table 1 for the synthetic natroalunite and Table 2 for the synthetic arsenic-incorporated natroalunite.

From the experimental results under the condition of initial pH 2.00 and 25°C, the solubility product [K_{sp}] and the Gibbs free energies of formation $\Delta G_f^\circ[Na_{0.93}(H_3O)_{0.61}Al_{2.82}(SO_4)_2(OH)_6]$ had been calculated to be $10^{-81.02\pm0.33}$ ~$10^{-81.04\pm0.27}$ and -4713 ± 2~-4714 ± 1 kJ/mol kJ/mol for the natroalunite correspondingly. Few K_{sp} and ΔG_f° data for natroalunite have been reported previously in the literature. For natroalunite ($NaAl_3(SO_4)_2(OH)_6$), the ΔG_f° value of

Table 1: Analytical data and solubility product of the synthetic natroalunite $[Na_{0.93}(H_3O)_{0.61}Al_{2.82}(SO_4)_2(OH)_6]$.

Temp (°C)	Initial pH	Time (h)	Analytical data (mmol/L)					$\log K_{sp}$	Average $\log K_{sp}$	ΔG_f° (kJ/mol)	Average ΔG_f° (kJ/mol)
			pH	Na	Al	AsO_4	SO_4				
		5760	4.08	9.961	1.448	0.000	4.991	−81.10		−4714	
25	2.00	6480	4.16	9.813	1.355	0.000	5.132	−80.77	−81.04 ± 0.27	−4712	−4714 ± 1
		7200	4.06	9.902	1.406	0.000	5.086	−81.25		−4715	
		5760	4.05	10.022	1.512	0.000	4.990	−81.20		−4714	
25	2.00	6480	4.17	10.054	1.376	0.000	5.157	−80.69	−81.02 ± 0.33	−4712	−4713 ± 2
		7200	4.07	10.013	1.444	0.000	5.061	−81.16		−4714	
		5760	4.38	6.494	0.100	0.000	3.918	−82.93		−4724	
25	4.00	6480	4.51	6.438	0.100	0.000	3.859	−82.23	−82.62 ± 0.39	−4720	−4723 ± 2
		7200	4.42	6.699	0.101	0.000	3.848	−82.69		−4723	
		5760	4.35	6.444	0.126	0.000	4.101	−82.82		−4724	
25	5.60	6480	4.57	6.392	0.128	0.000	3.998	−81.63	−82.34 ± 0.71	−4717	−4721 ± 4
		7200	4.39	6.398	0.127	0.000	4.004	−82.59		−4722	
		5760	4.03	13.332	1.099	0.000	5.253	−80.13			
35	2.00	6480	4.12	13.389	0.970	0.000	5.323	−79.81	−80.09 ± 0.28		
		7200	4.01	13.330	1.019	0.000	5.256	−80.33			
		5760	4.15	11.520	0.554	0.000	3.889	−78.91			
45	2.00	6480	4.24	11.620	0.604	0.000	4.039	−78.33	−78.73 ± 0.40		
		7200	4.13	11.549	0.586	0.000	3.990	−78.96			

Table 2: Analytical data and solubility product of the arsenic-incorporated natroalunite $[Na_{0.88}(H_3O)_{2.44}Al_{2.35}(AsO_4)_{0.38}(SO_4)_{1.62}](OH)_6$.

Temp (°C)	Initial pH	Time (h)	Analytical data (mmol/L)					$\log K_{sp}$	Average $\log K_{sp}$	ΔG_f° (kJ/mol)	Average ΔG_f° (kJ/mol)
			pH	Na	Al	AsO_4	SO_4				
		5760	3.98	16.477	0.666	0.161	6.744	−92.42		−5079	
25	2.00	6480	4.09	16.614	0.592	0.151	7.110	−92.00	−92.30 ± 0.30	−5077	−5078 ± 2
		7200	4.00	16.573	0.590	0.154	7.026	−92.47		−5079	
		5760	3.95	16.377	0.673	0.160	6.936	−92.59		−5080	
25	2.00	6480	4.08	16.531	0.596	0.151	7.007	−92.04	−92.41 ± 0.37	−5077	−5079 ± 2
		7200	3.96	16.466	0.630	0.155	6.950	−92.60		−5080	
		5760	4.88	13.771	0.015	0.106	7.634	−92.28		−5078	
25	4.00	6480	4.99	13.860	0.017	0.109	7.602	−91.67	−92.04 ± 0.37	−5075	−5077 ± 2
		7200	4.87	13.832	0.018	0.102	7.603	−92.15		−5078	
		5760	4.65	7.703	0.016	0.112	4.322	−93.21		−5084	
25	5.60	6480	4.73	7.760	0.016	0.111	4.238	−92.90	−93.16 ± 0.26	−5082	−5083 ± 2
		7200	4.62	7.601	0.016	0.108	4.394	−93.38		−5085	
		5760	3.70	11.048	1.011	0.204	4.746	−91.62			
35	2.00	6480	3.80	11.340	0.988	0.219	4.835	−91.10	−91.38 ± 0.28		
		7200	3.74	11.392	0.990	0.214	4.846	−91.42			
		5760	3.61	10.770	0.886	0.194	4.598	−90.53			
45	2.00	6480	3.74	11.057	0.835	0.190	4.653	−89.92	−90.36 ± 0.44		
		7200	3.61	11.011	0.819	0.196	4.684	−90.62			

−4614.02 kJ/mol was determined [48] from the K_{sp} value of $10^{79.7}$ [49]; besides, the ΔG_f° value of −4622.40 kJ/mol was presented [34].

The thermodynamic property of the arsenic-incorporated natroalunite has scarcely been examined previously. In the present work, with the arsenic incorporation increasing from 0% to 19%, the K_{sp} value for the arsenic-incorporated natroalunite decreased from $10^{-81.02\pm0.33}$ ~$10^{-81.04\pm0.27}$ to $10^{-92.30\pm0.30}$~$10^{-92.41\pm0.37}$, and the corresponding ΔG_f° values from −4713 ± 2 to −4714 ± 1 kJ/mol to −5078 ± 2 to −5079 ± 2 kJ/mol, respectively. Generally, the K_{sp} and ΔG_f° values for the natroalunite and the arsenic-incorporated natroalunite increased with the increasing dissolution temperature. They are also more soluble at initial pH of 2.00 than at initial pH of 4.00 and 5.60.

3.5. Determination of Thermodynamic Data. The solubility products (K_{sp}) for the synthetic natroalunite and the arsenic-incorporated natroalunite can also be estimated using the following equations [50]:

$$-\log K_{sp} = \frac{A}{T} + B + CT, \tag{13}$$

For the synthetic natroalunite (Natroal-1),

$$-\log K_{sp} = -\frac{60221.6658}{T} + 506.6639 - 0.7502T, \tag{14}$$

For the arsenic-incorporated natroalunite (As-Natroal-1).

$$-\log K_{sp} = -\frac{8175.9700}{T} + 175.2114 - 0.1860T, \tag{15}$$

For the arsenic-incorporated natroalunite (As-Natroal-2),

Table 3: Thermodynamic data of the natroalunite and the arsenic-incorporated natroalunite in aqueous acidic media (initial pH 2).

Sample	Temp (°C)	$\log K_{sp}$	ΔG° (J/K·mol)	ΔH° (J/mol)	ΔS° (J/K·mol)	ΔC_p° (J/K·mol)
Natroalunite	25	−81.03	462303.43	122466.83	−1140.39	4280.13
	35	−80.09	472271.06	209505.66	−853.13	4423.76
	45	−78.73	479366.12	299417.07	−565.88	4567.38
As-natroalunite	25	−92.35	526925.48	159674.76	−1232.38	1061.12
	35	−91.38	538893.25	181253.18	−1161.17	1096.72
	45	−90.36	550148.86	203543.76	−1089.95	1132.33

$$-\log K_{sp} = \frac{42272.1180}{T} - 127.3042 + 0.2916T. \quad (16)$$

The thermodynamic quantities ΔG°, ΔH°, ΔS°, and ΔC_p° for the dissolution of the synthetic natroalunite and the arsenic-incorporated natroalunite at initial pH 2.00 were estimated after equations (17)~(20) [50] and are given in Table 3:

$$\Delta G^\circ = 2.3026R\left(A + BT + CT^2\right), \quad (17)$$

$$\Delta H^\circ = 2.3026R\left(A - CT^2\right), \quad (18)$$

$$\Delta S^\circ = -2.3026R\left(B + 2CT\right), \quad (19)$$

$$\Delta C_p^\circ = -2.3026R\left(CT\right), \quad (20)$$

where A, B, and C are the empirical coefficients of equation (13).

The ΔG° values for the dissolution of the synthetic natroalunite and the synthetic arsenic-incorporated natroalunite increased with the temperature increase which showed that their dissolutions were energy expending processes [50]. The positive value of ΔH° indicated also that the dissolution was an endothermic reaction and the solubility increased with the increase in temperature. The higher ΔS° value for the natroalunite dissolution indicated that the order degree caused by SO_4^{2-} was greater than by AsO_4^{3-} in aqueous solution, which is related to the different bond distances (S-O 1.473 Å and As-O 1.682 Å) [50, 51]. The smaller SO_4^{2-} with a low charge can result in greater entropy, and consequently the synthetic natroalunite was more soluble than the arsenic-incorporated natroalunite in aqueous media. The higher ΔC_p° value coupled with the higher ΔS° value for the dissolution of the synthetic natroalunite in comparison to the corresponding values for the dissolution of the synthetic arsenic-incorporated natroalunite (Table 3) suggested a significant interaction of SO_4^{2-} with the aqueous acidic media and a higher solubility of the natroalunite in the aqueous acidic media. But the incorporation of H_3O^+ into the natroalunite crystal structure with the substitution of SO_4^{2-} by AsO_4^{3-} can increase the ΔS° values for the As-natroalunite dissolution and increase their solubility.

4. Conclusions

The lattice parameters were determined to be $a = 6.9870$ Å and $c = 16.5840$ Å for the synthetic natroalunite $[Na_{0.93}(H_3O)_{0.61}Al_{2.82}(SO_4)_2(OH)_6]$ and $a = 7.0016$ Å and $c = 16.7053$ Å for the synthetic arsenic-incorporated natroalunite $[Na_{0.88}(H_3O)_{2.44}Al_{2.35}(AsO_4)_{0.38}(SO_4)_{1.62}(OH)_6]$. The symmetric stretching vibration $\nu_1(AsO_4)$ around 895 cm^{-1} in the infrared spectra was recognized for the arsenic-incorporated natroalunite. The solids showed regular ditrigonal scalenohedron (pseudo-octahedron) crystal forms (2~5 μm size) with certain nanosized fine grains. The XRD, FT-IR. and FE-SEM characterization proved that the synthetic natroalunite and the arsenic-incorporated natroalunite showed no detectable changes during dissolution.

All dissolutions underwent a pH variation, which was caused by a great depleting of H_3O^+/OH^- ions, typically at the reaction beginning. The dissolution in H_3O^+ medium proved to be near-stoichiometric within the short beginning period and the dissolved Na^+, Al^{3+}, SO_4^{2-}, and AsO_4^{3-} concentrations were stoichiometric according to the initial solids and then appeared to be nonstoichiometric with the Na/SO_4 mole ratios higher and the Al/SO_4 and AsO_4/SO_4 mole ratios lower than the stoichiometry until the experimental end, indicating that the components were released from solid to solution preferentially after the following order: Na^+ $(H_3O^+) > SO_4^{2-} > AsO_4^{3-} > Al^{3+}$.

From the experimental results under the condition of initial pH 2.00 and 25°C, the solubility product $[K_{sp}]$ and the Gibbs free energies of formation $[\Delta G_f^\circ]$ were calculated to be $10^{-81.02\pm0.33}$~$10^{-81.04\pm0.27}$ and -4713 ± 2 to -4714 ± 1 kJ/mol kJ/mol for the natroalunite, $10^{-92.30\pm0.30}$~$10^{-92.41\pm0.37}$ and -5078 ± 2 to -5079 ± 2 kJ/mol for the arsenic-incorporated natroalunite, respectively. Thermodynamic quantities, ΔG°, ΔH°, ΔS°, and ΔC_p° were calculated to be 462303.43 J/K·mol, 122466.83 J/mol, −1140.39 J/K·mol, and 4280.13 J/K·mol for the natroalunite dissolution reaction at initial pH 2.00 and 25°C and to be 526925.48 J/K·mol, 159674.76 J/mol, −1232.38 J/K·mol, and 1061.12 J/K·mol for the dissolution reaction of the arsenic-incorporated natroalunite at initial pH 2.00 and 25°C, respectively.

Data Availability

The powder XRD data in XML format, the FT-IR data in XLSX format, and all solution analytical data in XLSX format used to support the findings of this study are available from the corresponding author upon request.

Conflicts of Interest

The authors declare that there are no conflicts of interest regarding the publication of this paper.

Acknowledgments

The authors are grateful for the financial support from the National Natural Science Foundation of China (41763012, 21707024, and 51978188), the Guangxi Science and Technology Planning Project (GuiKe-AD18126018), the Guangxi Natural Science Foundation (2018GXNSFAA050044), and the Special Fund for Guangxi Distinguished Experts.

References

[1] P. L. Smedley and D. G. Kinniburgh, "A review of the source, behaviour and distribution of arsenic in natural waters," *Applied Geochemistry*, vol. 17, no. 5, pp. 517–568, 2002.

[2] M. A. Davis, A. J. Signes-Pastor, M. Argos et al., "Assessment of human dietary exposure to arsenic through rice," *Science of The Total Environment*, vol. 586, no. 5, pp. 1237–1244, 2017.

[3] X. He, M. R. Karagas, and C. Murray, "Impact of receipt of private well arsenic test results on maternal use of contaminated drinking water in a U.S. population," *Science of The Total Environment*, vol. 643, no. 12, pp. 1005–1012, 2018.

[4] Z. Wang, H. Guo, W. Xiu, J. Wang, and M. Shen, "High arsenic groundwater in the Guide basin, northwestern China: distribution and genesis mechanisms," *Science of The Total Environment*, vol. 640-641, no. 11, pp. 194–206, 2018.

[5] A. M. Nazari, R. Radzinski, and A. Ghahreman, "Review of arsenic metallurgy: treatment of arsenical minerals and the immobilization of arsenic," *Hydrometallurgy*, vol. 174, no. 12, pp. 258–281, 2017.

[6] Y. Li, Y. Zhu, Z. Zhu, X. Zhang, D. Wang, and L. Xie, "Fixed-bed column adsorption of arsenic(V) by porous composite of magnetite/hematite/carbon with eucalyptus wood microstructure," *Journal of Environmental Engineering and Landscape Management*, vol. 26, no. 1, pp. 38–56, 2018.

[7] Y. Zhu, Z. Jiang, Z. Zhu, H. Liu, L. Zhang, and J. Lin, "Arsenic immobilization from aqueous solution by the precipitation of the pseudo-octahedral arsenate-substituted natroalunite solid solutions," *Science of The Total Environment*, vol. 669, no. 6, pp. 754–766, 2019.

[8] R. G. Robins, "The solubility of barium arsenate: sherritt's barium arsenate process," *Metallurgical Transactions B*, vol. 16, no. 2, pp. 404–406, 1985.

[9] T. Nishimura and R. G. Robins, "A re-evaluation of the solubility and stability regions of calcium arsenites and calcium arsenates in aqueous solution at 25°C," *Mineral Processing and Extractive Metallurgy Review*, vol. 18, no. 3-4, pp. 283–308, 1998.

[10] J. V. Bothe and P. W. Brown, "Arsenic immobilization by calcium arsenate formation," *Environmental Science & Technology*, vol. 33, no. 21, pp. 3806–3811, 1999.

[11] M. C. F. Magalhães, "Arsenic. An environmental problem limited by solubility," *Pure and Applied Chemistry*, vol. 74, no. 10, pp. 1843–1850, 2002.

[12] Y. Zhu, X. Zhang, Q. Xie, D. Wang, and G. Cheng, "Solubility and stability of calcium arsenates at 25°C," *Water, Air, & Soil Pollution*, vol. 169, no. 1-4, pp. 221–238, 2006.

[13] D. Langmuir, J. Mahoney, and J. Rowson, "Solubility products of amorphous ferric arsenate and crystalline scorodite ($FeAsO_4{\cdot}2H_2O$) and their application to arsenic behavior in buried mine tailings," *Geochimica et Cosmochimica Acta*, vol. 70, no. 12, pp. 2942–2956, 2006.

[14] D. Paktunc and K. Bruggeman, "Solubility of nanocrystalline scorodite and amorphous ferric arsenate: implications for stabilization of arsenic in mine wastes," *Applied Geochemistry*, vol. 25, no. 5, pp. 674–683, 2010.

[15] M. C. Bluteau and G. P. Demopoulos, "The incongruent dissolution of scorodite—solubility, kinetics and mechanism," *Hydrometallurgy*, vol. 87, no. 3-4, pp. 163–177, 2007.

[16] J. Viñals, A. Sunyer, P. Molera, M. Cruells, and N. Llorca, "Arsenic stabilization of calcium arsenate waste by hydrothermal precipitation of arsenical natroalunite," *Hydrometallurgy*, vol. 104, no. 2, pp. 247–259, 2010.

[17] F. L. Pantuzzo, L. R. G. Santos, and V. S. T. Ciminelli, "Solubility-product constant of an amorphous aluminum-arsenate phase ($AlAsO_4{\cdot}3.5H_2O$) AT 25°C," *Hydrometallurgy*, vol. 144-145, no. 4, pp. 63–68, 2014.

[18] M. A. Gomez, L. Becze, J. N. Cutler, and G. P. Demopoulos, "Hydrothermal reaction chemistry and characterization of ferric arsenate phases precipitated from $Fe_2(SO_4)_3$-As_2O_5-H_2SO_4 solutions," *Hydrometallurgy*, vol. 107, no. 3-4, pp. 74–90, 2011.

[19] S. A. Welch, D. Kirste, A. G. Christy, F. R. Beavis, and S. G. Beavis, "Jarosite dissolution II—reaction kinetics, stoichiometry and acid flux," *Chemical Geology*, vol. 254, no. 1-2, pp. 73–86, 2008.

[20] J. L. Miller, A. S. Elwood Madden, C. M. Phillips-Lander, B. N. Pritchett, and M. E. Elwood Madden, "Alunite dissolution rates: dissolution mechanisms and implications for Mars," *Geochimica et Cosmochimica Acta*, vol. 172, no. 1, pp. 93–106, 2016.

[21] A. M. L. Smith, K. A. Hudson-Edwards, W. E. Dubbin, and K. Wright, "Dissolution of jarosite $[KFe_3(SO_4)_2(OH)_6]$ at pH 2 and 8: insights from batch experiments and computational modelling," *Geochimica et Cosmochimica Acta*, vol. 70, no. 3, pp. 608–621, 2006.

[22] U. Kolitsch and A. Pring, "Crystal chemistry of the crandallite, beudantite and alunite groups: a review and evaluation of the suitability as storage materials for toxic metals," *Journal of Mineralogical and Petrological Sciences*, vol. 96, no. 2, pp. 67–78, 2001.

[23] D. Paktunc and J. E. Dutrizac, "Characterization of arsenate-for-sulfate substitution in synthetic jarosite using X-ray diffraction and X-ray absorption spectroscopy," *The Canadian Mineralogist*, vol. 41, no. 4, pp. 905–919, 2003.

[24] P. J. Murphy, A. M. L. Smith, K. A. Hudson-Edwards, W. E. Dubbin, and K. Wright, "Raman and IR spectroscopic studies of alunite-supergroup compounds containing Al, Cr^{3+}, Fe^{3+} and V^{3+} at the B site," *The Canadian Mineralogist*, vol. 47, no. 3, pp. 663–681, 2009.

[25] S. A. Welch, A. G. Christy, D. Kirste, S. G. Beavis, and F. Beavis, "Jarosite dissolution I—trace cation flux in acid sulfate soils," *Chemical Geology*, vol. 245, no. 3-4, pp. 183–197, 2007.

[26] K. S. Savage, D. K. Bird, and P. A. O'Day, "Arsenic speciation in synthetic jarosite," *Chemical Geology*, vol. 215, no. 1–4, pp. 473–498, 2005.

[27] A. Sunyer and J. Viñals, "Arsenate substitution in natroalunite: a potential medium for arsenic immobilization. Part 1: synthesis and compositions," *Hydrometallurgy*, vol. 109, no. 1-2, pp. 54–64, 2011.

[28] A. Sunyer and J. Viñals, "Arsenate substitution in natroalunite: a potential medium for arsenic immobilization. Part 2: cell parameters and stability tests," *Hydrometallurgy*, vol. 109, no. 1-2, pp. 106–115, 2011.

[29] A. Sunyer, M. Currubí, and J. Viñals, "Arsenic immobilization as alunite-type phases: the arsenate substitution in alunite and

hydronium alunite," *Journal of Hazardous Materials*, vol. 261, no. 10, pp. 559–569, 2013.

[30] Z. Q. Luo, X. T. Zhou, Q. M. Jia, X. F. Chen, Z. C. Tao, and S. Q. Liu, "Preparation of arsenical-natroalunite solid solutions with high crystallinity by hydrothermal method," *Materials Research Innovations*, vol. 19, no. 6, pp. 26–29, 2015.

[31] D. L. Parkhurst and C. A. J. Appelo, "Description of input and examples for PHREEQC version 3—a computer program for speciation, batch-reaction, one-dimensional transport, and inverse geochemical calculations," in *U.S. Geological Survey Techniques and Methods, Book 6, Chapter A43*, pp. 1–497, 2013.

[32] J. D. Allison, D. S. Brown, and K. J. Novo-Gradac, *MINTEQA2/PRODEFA2, a Geochemical Assessment Model for Environmental Systems: Version 3.0 User's Manual*, Environmental Research Laboratory, Office of Research and Development, U.S. Environmental Protection Agency, Athens, GA, USA, 1991.

[33] U.S. Environmental Protection Agency, *MINTEQA2/PRODEFA2, a Geochemical Assessment Model for Environmental Systems: User Manual Supplement for Version 4.0*, National Exposure Research Laboratory, Ecosystems Research Division, Athens, GA, USA, 1998.

[34] R. E. Stoffregen and G. L. Cygan, "An experimental study of Na-K exchange between alunite and aqueous sulfate solutions," *American Mineralogist*, vol. 75, no. 1-2, pp. 209–220, 1990.

[35] L. C. Basciano and R. C. Peterson, "Crystal chemistry of the natrojarosite-jarosite and natrojarosite-hydronium jarosite solid-solution series: a synthetic study with full Fe site occupancy," *American Mineralogist*, vol. 93, no. 5-6, pp. 853–862, 2008.

[36] E. Sato, I. Nakai, R. Miyawaki, and S. Matsubara, "Crystal structures of alunite family minerals: beaverite, corkite, alunite, natroalunite, jarosite, svanbergite, and woodhouseite," *Neues Jahrbuch für Mineralogie-Abhandlungen*, vol. 185, no. 3, pp. 313–322, 2009.

[37] D. Baron and C. D. Palmer, "Solubility of jarosite at 4–35°C," *Geochimica et Cosmochimica Acta*, vol. 60, no. 2, pp. 185–195, 1996.

[38] J. L. Bishop and E. Murad, "The visible and infrared spectral properties of jarosite and alunite," *American Mineralogist*, vol. 90, no. 7, pp. 1100–1107, 2005.

[39] S. K. Zahrai, M. E. Elwood Madden, A. S. Madden, and J. D. Rimstidt, "Na-jarosite dissolution rates: the effect of mineral composition on jarosite lifetimes," *Icarus*, vol. 223, no. 1, pp. 438–443, 2013.

[40] M. E. Elwood Madden, A. S. Madden, J. D. Rimstidt, S. Zahrai, M. R. Kendall, and M. A. Miller, "Jarosite dissolution rates and nanoscale mineralogy," *Geochimica et Cosmochimica Acta*, vol. 91, no. 8, pp. 306–321, 2012.

[41] M. R. Kendall, A. S. Madden, M. E. Elwood Madden, and Q. Hu, "Effects of arsenic incorporation on jarosite dissolution rates and reaction products," *Geochimica et Cosmochimica Acta*, vol. 112, no. 7, pp. 192–207, 2013.

[42] P. Acero, K. A. Hudson-Edwards, and J. D. Gale, "Influence of pH and temperature on alunite dissolution: rates, products and insights on mechanisms from atomistic simulation," *Chemical Geology*, vol. 419, no. 12, pp. 1–9, 2015.

[43] B. Gasharova, J. Göttlicher, and U. Becker, "Dissolution at the surface of jarosite: an in situ AFM study," *Chemical Geology*, vol. 215, no. 1–4, pp. 499–516, 2005.

[44] M. T. Fulmer, I. C. Ison, C. R. Hankermayer, B. R. Constantz, and J. Ross, "Measurements of the solubilities and dissolution rates of several hydroxyapatites," *Biomaterials*, vol. 23, no. 3, pp. 751–755, 2002.

[45] I. A. Reyes, I. Mireles, F. Patiño et al., "A study on the dissolution rates of K-Cr(VI)-jarosites: kinetic analysis and implications," *Geochemical Transactions*, vol. 17, no. 3, pp. 1–18, 2016.

[46] W. Stumm and J. J. Morgan, *Aquatic Chemistry, Chemical Equilibria and Rates in Natural Waters*, John Wiley & Sons, New York, NY, USA, 1996.

[47] D. K. Nordstrom, J. Majzlan, and E. Konigsberger, "Thermodynamic properties for arsenic minerals and aqueous species," *Reviews in Mineralogy and Geochemistry*, vol. 79, no. 1, pp. 217–255, 2014.

[48] J. Prietzel and B. Mayer, "Isotopic fractionation of sulfur during formation of basaluminite, alunite, and natroalunite," *Chemical Geology*, vol. 215, no. 1–4, pp. 525–535, 2005.

[49] D. K. Nordstrom, "The effect of sulfate on aluminum concentrations in natural waters: some stability relations in the system Al_2O_3-SO_3-H_2O at 298 K," *Geochimica et Cosmochimica Acta*, vol. 46, no. 4, pp. 681–692, 1982.

[50] P. P. Mahapatra, H. Mishra, and N. S. Chickerur, "Solubility and thermodynamic data of cadmium hydroxyapatite in aqueous media," *Thermochimica Acta*, vol. 54, no. 1-2, pp. 1–8, 1982.

[51] F. Patiño, I. A. Reyes, M. U. Flores et al., "Kinetic modeling and experimental design of the sodium arsenojarosite decomposition in alkaline media: Implications," *Hydrometallurgy*, vol. 137, no. 5, pp. 115–125, 2013.